

Thermodynamics and electronic structure characteristics of MFe_2O_4 with different spinel structures: A first-principles study

Guanting Liu¹, Jiaju Wang¹, Xiaoli Sheng, Xuyan Xue^{**}, Yiqian Wang^{*}

College of Physics, Qingdao University, No. 308, Ningxia Road, Qingdao, 266071, PR China

ARTICLE INFO

Handling Editor: Dr P. Vincenzini

Keywords:

First-principles calculation
Spinel ferrites
Thermodynamics
Electronic structure

ABSTRACT

In recent years, spinel ferrites with chemical formula MFe_2O_4 , have attracted much attention due to their impressive photocatalytic and electrocatalytic performances, which are significantly influenced by their spinel structures. However, it is still a big challenge to distinguish or predict spinel structures for spinel ferrites. As an attempt to address this issue, this paper presents a first-principles study of the thermodynamics and electronic structures for six spinel ferrites with different spinel structures. The configurational free energy of these spinel ferrites at different inversion degrees is calculated to determine the equilibrium inversion degree for each spinel, which successfully predicts the spinel structure type of these spinel ferrites. The partial density of states is obtained for six spinel ferrites assuming they are normal or inverse spinels. The electronic states close to the Fermi energy of each spinel ferrite are carefully examined, showing that normal spinels have weak interactions between M and Fe states, while strong interactions exist in mixed or inverse spinels. Our results offer an insightful understanding of different spinel structures, and provide a reliable approach to determine the spinel structure of spinel ferrites.

1. Introduction

Recently, spinel ferrites, with chemical formula MFe_2O_4 , have attracted the spotlight of the catalysis research field. Spinel ferrites have major applications in Fenton-type catalysis [1], photocatalysis [2] and electrocatalysis [3] due to their low cost, high corrosion resistance, and diverse physicochemical properties [4–6]. These catalytic applications are closely related to conductivity, optical transition and electronic structure of spinel ferrites [7,8], which are greatly influenced by the spinel structures. Thus, to achieve better catalytic performances of spinel ferrites, it is imperative to differentiate their spinel structures and investigate their electronic structures.

Spinel structures are categorized into normal, mixed, and inverse according to cation distributions at octahedral and tetrahedral sites. To identify the spinel structure, it is key to determine the cation distribution in spinels. Researchers have proposed several methods to predict the cation distribution. Initially, crystal-field stabilization energies (CFSE) were used to obtain octahedral site stabilization energy (OSSE) as a function of d -orbital electron number, and the cation with lower OSSE

was thought to preferentially occupy the octahedral sites. Other factors that were found to influence the cation distribution included the electronic configuration, the electrostatic energy of the lattice, the short-range Born repulsion energy, and polarization effects [9,10]. Nevertheless, none of these factors could be used to obtain the cation distribution of a spinel independently. Later in 1982, Burdett et al. made an effort to determine the cation distribution in spinels by comparing the sizes of s and p atomic orbitals of cations [11]. This method was successful in predicting many spinel structures, but the spinel structures of ferrites $CdFe_2O_4$ and $MnFe_2O_4$ were not correctly identified. More recently, researchers have used configurational thermodynamics to predict the cation distribution of spinels [12–14], but this method has not been implemented on classification of spinel ferrites. Although progress has been made on determination of cation distribution in spinels, no generalized rules have been found for spinel ferrites. Thus, a reliable method to identify the spinel structure of a spinel ferrite is urgently needed.

Recently, density functional theory (DFT) has been widely used to calculate the partial density of states (PDOS) of spinels [14–20]. Though

* Corresponding author.

** Corresponding author.

E-mail addresses: xuexy@qdu.edu.cn (X. Xue), yqwang@qdu.edu.cn (Y. Wang).

¹ These authors contributed to this work equally.

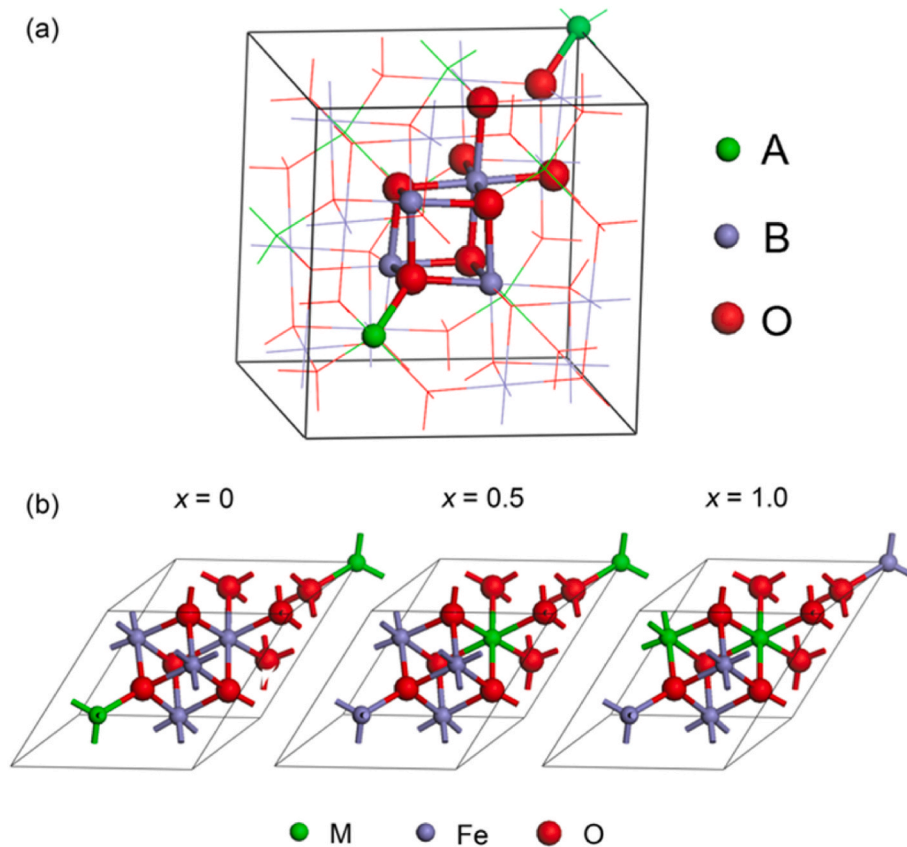


Fig. 1. (a) Schematics of a full unit cell of a perfect spinel. (b) Schematics of three primitive unit cells of the $(M_{1-x}Fe_x)_A(M_xFe_{2-x})_B O_4$ spinels ($x = 0, 0.5$ and 1.0).

electronic structure of spinels can be significantly affected by their spinel structures, little effort was devoted to identifying the structure type of spinel ferrites using PDOS. In previous PDOS calculations for spinel ferrites, some found that the bands near the Fermi energy (E_F) have major contributions from O electronic states [15,16], while others thought that dominant contributions near E_F were from Fe and M states [17,18]. For example, Szotek et al. [16] demonstrated that the valence band of $MnFe_2O_4$ is predominantly of the oxygen type, but Rafiq et al. [17] showed that O DOS near E_F of $MnFe_2O_4$ is very low. In these studies, it was found that the energy of O DOS with respect to E_F is inconsistent, which requires further investigation. To identify spinel structures using PDOS, a feasible approach would be to compare PDOS of spinel ferrites with different spinel structures. However, only a few studies tried to implement this idea on identification of spinel structure for MFe_2O_4 ($M = Mn, Fe, Co, Ni$ [16]; $M = Mn, Co, Ni$ [17]), and no specific patterns were derived from the PDOS for spinel ferrites with different spinel structures. Therefore, a systematic investigation should be carried out to search for a pattern from the PDOS of spinel ferrites with different spinel structures.

To improve on previous efforts, this work attempts to differentiate spinel ferrite structures using first-principles calculations. The

thermodynamics and electronic structures of six spinel ferrites with different spinel structures (normal: $CdFe_2O_4$ and $ZnFe_2O_4$; mixed: $MgFe_2O_4$ and $MnFe_2O_4$; inverse: $NiFe_2O_4$ and $CoFe_2O_4$) were studied. Their thermodynamic distinctions and electronic structure characteristics were examined, and correlated with their spinel structures.

2. Calculation details

Spin-polarized quantum mechanical calculations were carried out using DFT as implemented in the Vienna *ab initio* simulation package (VASP). The projector augmented wave pseudopotential method (PAW) was used to accurately describe the structure optimization and the electron-ion interaction in the density of states (DOS). The generalized gradient approximation (GGA) functional (PW91) was used to treat the electron-electron interaction potentials with exchange and correlation functionals. For MFe_2O_4 ($M = Mg, Mn, Co, Ni, Zn$ and Cd), the valence electrons of these atoms are denoted by Fe: $3d^7 4s^1$, O: $2s^2 2p^4$, Mg: $3s^2$, Mn: $3d^6 4s^1$, Co: $3d^8 4s^1$, Ni: $3d^8 4s^2$, Zn: $3d^{10} 4s^2$, Cd: $4d^{10} 5s^2$. The kinetic energy cutoff for the plane-wave basis set expansion was set at 400 eV for the geometry optimizations to avoid the Pulay stress arising from the cell shape relaxations. A Γ -centered Monkhorst-Pack grid of $5 \times 5 \times 5$ k

Table 1

Summary of the initial unit cell lattice (a_0) of MFe_2O_4 spinels, the relaxed lattice parameter (a) for $x = 0, 0.5$, and 1.0 , and the lattice parameter difference (Δa).

Spinel	a_0 (Å)	a (Å)			$\Delta a = a - a_0$ (Å)		
	Experimental	$x = 0$	$x = 0.5$	$x = 1.0$	$x = 0$	$x = 0.5$	$x = 1.0$
$ZnFe_2O_4$	8.4411 [23]	8.1169	8.2024	8.1426	-0.3242	-0.2387	-0.2985
$CdFe_2O_4$	8.6996 [24]	8.4103	8.9398	8.4180	-0.2893	0.2402	-0.2816
$CoFe_2O_4$	8.3919 [25]	7.9939	8.0579	7.9969	-0.3980	-0.3340	-0.3950
$NiFe_2O_4$	8.3390 [26]	8.0221	8.1040	8.0295	-0.3169	-0.2350	-0.3095
$MgFe_2O_4$	8.3750 [27]	8.1221	8.1337	8.0726	-0.2529	-0.2413	-0.3024
$MnFe_2O_4$	8.4990 [28]	8.0085	7.8983	8.0139	-0.4905	-0.6007	-0.4851

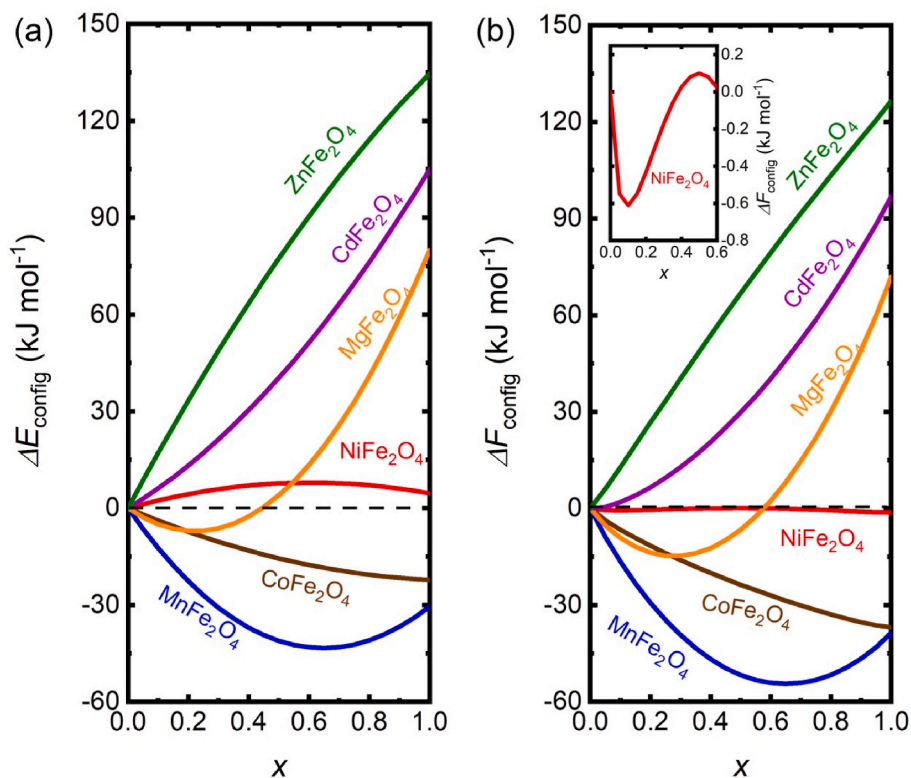


Fig. 2. (a) Configurational inversion energy (ΔE_{config}) and (b) configurational inversion free energy (ΔF_{config}) as a function of the inversion degree for $M\text{Fe}_2\text{O}_4$. The inset in (b) shows enlargement of ΔF_{config} for the NiFe_2O_4 spinels for $x = 0\text{--}0.6$.

points was used for all calculations. During relaxation, Feynman forces on each atom were minimized until they were less than $0.01 \text{ eV } \text{\AA}^{-1}$. For the calculation of the DOS we applied the tetrahedral method with Blöch corrections. Atomic charges were analyzed using the Bader partition methodology [21].

Fig. 1(a) shows a full unit cell of $M\text{Fe}_2\text{O}_4$ containing 4 rhombohedral primitive unit cells, which contains 14 atoms. Denoting tetrahedral sites as A, and octahedral sites as B, we can write the spinel ferrite chemical formula as $(M_{1-x}\text{Fe}_x)_A(M_x\text{Fe}_{2-x})_B\text{O}_4$, where x is the inversion degree. Experimental lattice parameters (a_0) were adopted as the lattice parameters for the starting structures of the spinel ferrites, which can be found in Table 1. Calculations were performed for three x values, *i.e.*, 0, 0.5, and 1.0, whose unit-cell schematics are shown in Fig. 1(b). Under these circumstances, the site occupancy artificially lowers the symmetry from space group $Fd\bar{3}m$ (No. 227) in the normal spinel to $R3m$ (No. 160) in the half-inverted spinel and to $Imma$ (No. 74) in the inverse spinel. The use of the primitive cell ensures that there is a single cation configuration for each of these three inversion degrees, which simplifies the simulations, allowing us to efficiently carry out calculations for six spinel ferrites.

The calculation of the thermodynamic quantities at different inversion degrees in spinels containing two different cations is modified from the thermodynamic considerations of Navrotsky and Kleppa [22]. This methodology is based on the treatment of the spinels' cation distribution as a chemical equilibrium. The configurational free energy of inversion per formula unit, ΔF_{config} , is given by

$$\Delta F_{\text{config}} = \Delta E_{\text{config}} - T \Delta S_{\text{config}} \quad (1)$$

where ΔE_{config} is the configurational inversion energy per formula unit, T is the temperature, and ΔS_{config} is the ideal configurational entropy per formula unit.

The internal energy, E_x , is approximated using a quadratic formula of x given by [13].

$$E_x = ax^2 + bx \quad (2)$$

where the coefficients a and b can be evaluated using the predicted internal energies at inversion degrees 0.5 and 1. E_x at a certain x value can then be interpolated using the quadratic equation. ΔE_{config} at inversion degree x is then given by $E_x - E_0$.

The ideal configurational entropy per formula unit, ΔS_{config} , is calculated as [22].

$$\Delta S_{\text{config}} = -R [x \ln x + (1-x) \ln(1-x) + x \ln(x/2) + (2-x) \ln(1-x/2)] \quad (3)$$

where R is the ideal gas constant. $\Delta S_{\text{config}} = 0$ and $11.53 \text{ J mol}^{-1} \text{ K}^{-1}$ for $x = 0$ and 1, respectively, and reaches the maximum value $15.88 \text{ J mol}^{-1} \text{ K}^{-1}$ for the completely random distribution at $x = 2/3$. In Eqs. (1) and (3), ΔE_{config} and ΔS_{config} represent only configurational changes, in accordance with previous work [12–14]. Vibrational contributions are ignored as they are typically small compared to configurational changes in E and S [12].

3. Results and discussion

3.1. Equilibrium structures of $M\text{Fe}_2\text{O}_4$

The lattice parameters and internal coordinates were fully optimized for each inversion degree. The primitive cell shape was kept perfectly rhombohedral in such a way that the conventional cell was always cubic. Table 1 shows the optimized lattice parameters for $x = 0, 0.5$, and 1.0. The optimized lattice parameters are within 6% of a_0 . Except for the $x = 0.5$ scenario of CdFe_2O_4 , all relaxed lattice parameters are smaller than the experimental ones. Moreover, except for MnFe_2O_4 , the a value at $x = 0.5$ is larger compared to those at $x = 0$ and 1 for each spinel ferrite. It can be seen that a values vary with different inversion degrees, although no generalized rule can be derived from Table 1.

Table 2

Bader charges in units of e^- for atoms in MFe_2O_4 at $x = 0$ and 1. A denotes tetrahedral sites. B_{Fe} and B_M denote octahedral sites occupied by Fe and M atoms, respectively.

Spinel	x	A	B_{Fe}	B_M	O
ZnFe ₂ O ₄	0	1.388	1.696	–	–1.195
ZnFe ₂ O ₄	1	1.575	1.661	1.390	–1.156
CdFe ₂ O ₄	0	1.276	1.611	–	–1.125
CdFe ₂ O ₄	1	1.707	1.643	1.276	–1.156
CoFe ₂ O ₄	0	1.294	1.612	–	–1.129
CoFe ₂ O ₄	1	1.646	1.625	1.421	–1.173
NiFe ₂ O ₄	0	1.211	1.718	–	–1.162
NiFe ₂ O ₄	1	1.658	1.655	1.365	–1.170
MgFe ₂ O ₄	0	2.000	1.693	–	–1.346
MgFe ₂ O ₄	1	1.583	1.627	2.000	–1.302
MnFe ₂ O ₄	0	1.772	1.600	–	–1.243
MnFe ₂ O ₄	1	1.527	1.534	1.781	–1.210

3.2. Thermodynamic analysis

In Fig. 2(a), the configurational inversion energy of MFe_2O_4 per formula unit (ΔE_{config}) was plotted against the inversion degree (x) using a quadratic curve. For ZnFe₂O₄ and CdFe₂O₄, ΔE_{config} monotonically increases with x , and their minima are at $x = 0$. For MgFe₂O₄ and MnFe₂O₄, ΔE_{config} decreases, and then increases, reaching the minimum at $x = 0.2$ and $x = 0.65$, respectively. For NiFe₂O₄, ΔE_{config} increases, and then decreases, with a maximum of 7.9 kJ mol^{-1} at $x = 0.6$, and minimum at $x = 0$. For CoFe₂O₄, ΔE_{config} monotonically decreases with x ,

with its minimum at $x = 1$. Apart from NiFe₂O₄, the x values corresponding to the minimum of ΔE_{config} correctly predict the spinel structure type of these ferrites in the ground state. Therefore, further calculation of the configurational free energy is required.

Fig. 2(b) shows the relationship of ΔF_{config} and inversion degree of the investigated spinel ferrites. The configurational free energy (ΔF_{config}) of inversion was estimated at a typical calcination temperature of 700 K. For NiFe₂O₄, the temperature was set at 500 K considering its low preparation temperatures reported [29,30]. For each spinel ferrite, the equilibrium inversion degree is the x value corresponding to the minimum of the ΔF_{config} . For ZnFe₂O₄ and CdFe₂O₄, the minima of their ΔF_{config} curves are at $x = 0$, hence we deduce they are normal spinels, consistent with experimental results [31,32]. For NiFe₂O₄, although a local minimum of ΔF_{config} is found at $x = 0.1$, which might be related to a metastable state [14], the global minimum is at $x = 1$. For CoFe₂O₄, ΔF_{config} also has its minimum at $x = 1$. Therefore, the thermodynamic calculations show NiFe₂O₄ and CoFe₂O₄ are inverse spinels, which agrees with experimental results [30,33]. For MgFe₂O₄ and MnFe₂O₄, the x values corresponding to the ΔF_{config} minima are $x_{\text{min}} = 0.3$ and $x_{\text{min}} = 0.65$, respectively. Their ΔF_{config} minima are between $x = 0$ and $x = 1$, hence they are mixed spinels. For the mixed spinels, their spinel structure type is correctly predicted, but the equilibrium inversion degrees differ from experimental values, i.e., $x \sim 0.9$ for MgFe₂O₄ [34,35] and $x \sim 0.2$ for MnFe₂O₄ [36,37]. From above analysis, we conclude that the thermodynamic free energy approach can successfully predict the spinel structures of above spinel ferrites, although the theoretical prediction of inversion degree does not agree well with experimental

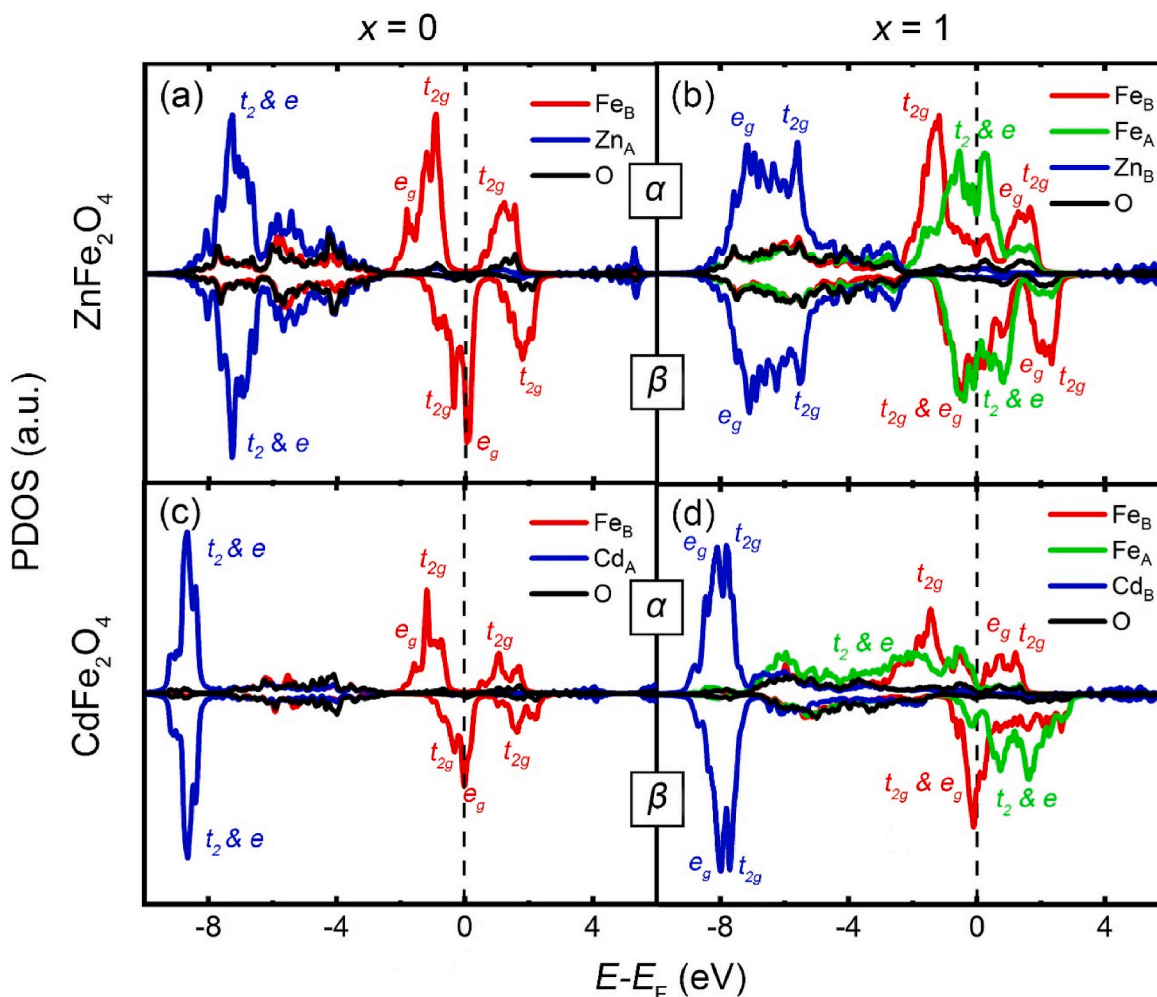


Fig. 3. PDOS per atom for ZnFe₂O₄ and CdFe₂O₄ at inversion degrees 0 and 1.

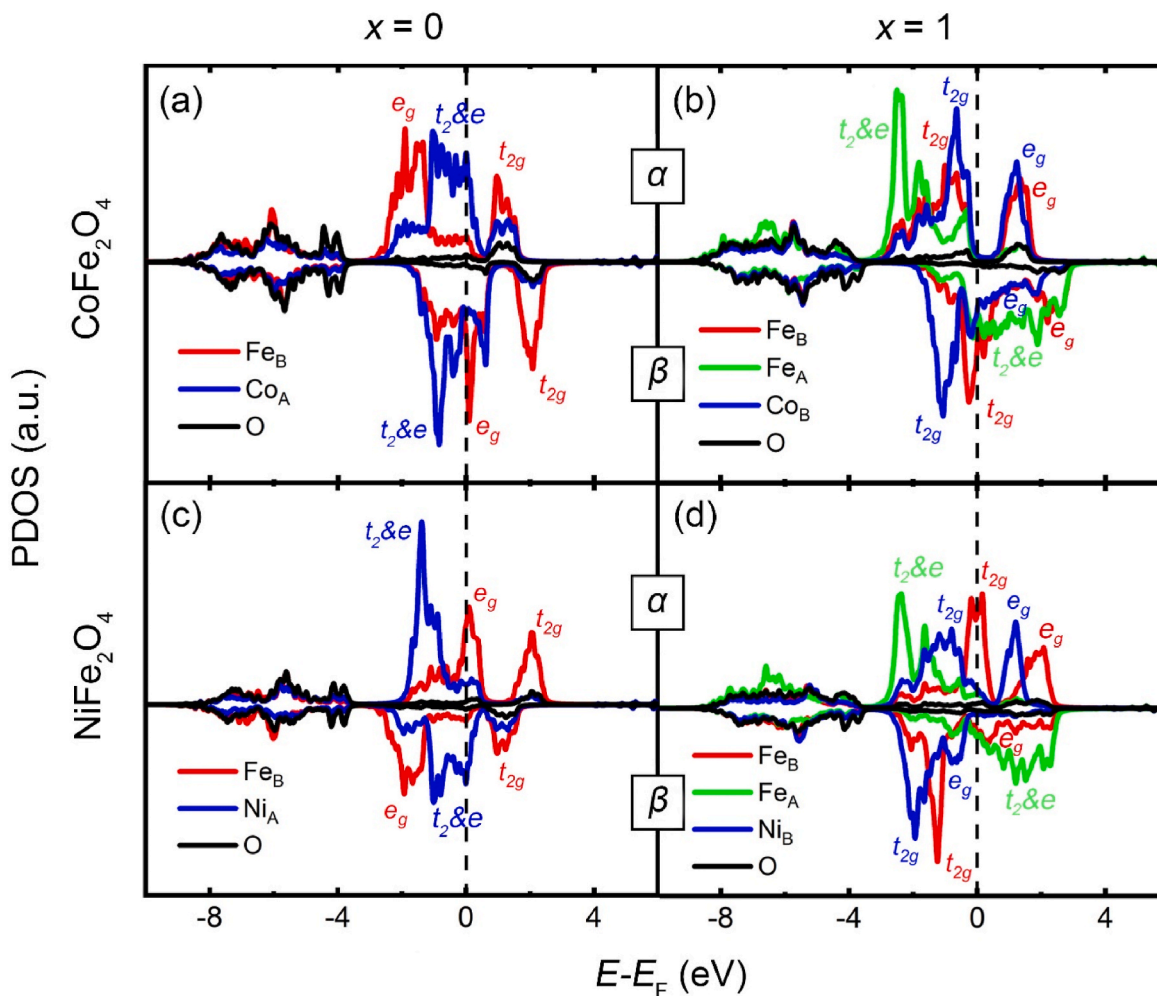


Fig. 4. PDOS per atom for CoFe_2O_4 and NiFe_2O_4 at inversion degrees 0 and 1.

values for the mixed ones.

In previous thermodynamic calculations on spinel ferrites, it was found that the variation of inversion degree was only taken into account for MgFe_2O_4 [38] and CoFe_2O_4 [39]. Unlike our configurational entropy and energy, in these calculations, entropy and enthalpy changed with temperature, with fixed values used in certain temperature ranges. For MgFe_2O_4 [38] and CoFe_2O_4 [39], their equilibrium inversion degrees were considered to be 1 at low temperatures, and decreased with increasing temperature, reaching ~ 0.92 and ~ 0.90 at 700 K, respectively. The inversion degree of MgFe_2O_4 in previous study [38] is closer to the experimental one than ours, indicating that further consideration of the temperature dependence of these thermodynamic quantities may be required.

3.3. Bader charge

The Bader charges of spinel ferrites at inversion degrees 0 and 1 are listed in Table 2. A high Bader charge means the atom is close to the perfect ion. In Table 2, all calculated Bader charges are less than the charges gained or lost in ideal ions (Fe^{3+} , M^{2+} and O^{2-}), with the strongly ionic Mg^{2+} as an exception. This underestimation was also reported in previous literature [14]. Depending on the ferrite, switching from A to B sites could have different effects on Bader charges of Fe and M atoms. For example, the Bader charge of Fe at A site is lower than that at B sites for ZnFe_2O_4 , but the opposite is true for CdFe_2O_4 . An interesting observation is that the ionic nature of M and O for mixed spinels is stronger than that of normal and inverse spinels. For CoFe_2O_4 and

NiFe_2O_4 , the Bader charge of M atoms at B sites is about 10% higher than that at A sites. This suggests that M atoms are more ionic and more stable when occupying B sites, thus indicating that CoFe_2O_4 and NiFe_2O_4 are inverse spinels.

3.4. Electronic PDOS of MFe_2O_4

Calculations of the electronic PDOS per atom were carried out for the investigated spinel ferrites at inversion degrees 0 and 1.

Fig. 3 shows the PDOS for ZnFe_2O_4 and CdFe_2O_4 at inversion degrees 0 and 1. For M and Fe atoms, only the outer shell *d* electrons were considered. The Jahn-Teller effect causes splitting of the 3*d* states. At octahedral sites, the split states are denoted by t_{2g} and e_g . At tetrahedral sites, the split states are labelled differently as t_2 and e . From Fig. 3, it can be seen that most O states have low energies between -3.0 and -8.0 eV. In addition, a few states of Fe appear in this energy range, which are hybridized with O 2*p* orbitals.

When $x = 0$, in both spinels, the Fe β channel states pass through E_F while Fe α channel states form a gap near E_F . For Fe β states, e_g states are located between two t_{2g} bands, while Fe α states have e_g states lower in energy than t_{2g} states. For M states, the t_2 and e states, which are close in energy, lie far below E_F . When $x = 1$, for both spinels, the overall distribution of Fe β states is analogous to that of $x = 0$, but the e_g and t_{2g} states are closer in energy and harder to distinguish. Fe α states show different characteristics in the two spinels. For ZnFe_2O_4 , Fe α states are symmetrical and most have energies between -2.0 and $+2.0$ eV, passing through E_F . For CdFe_2O_4 , α channel states of Fe α , which are

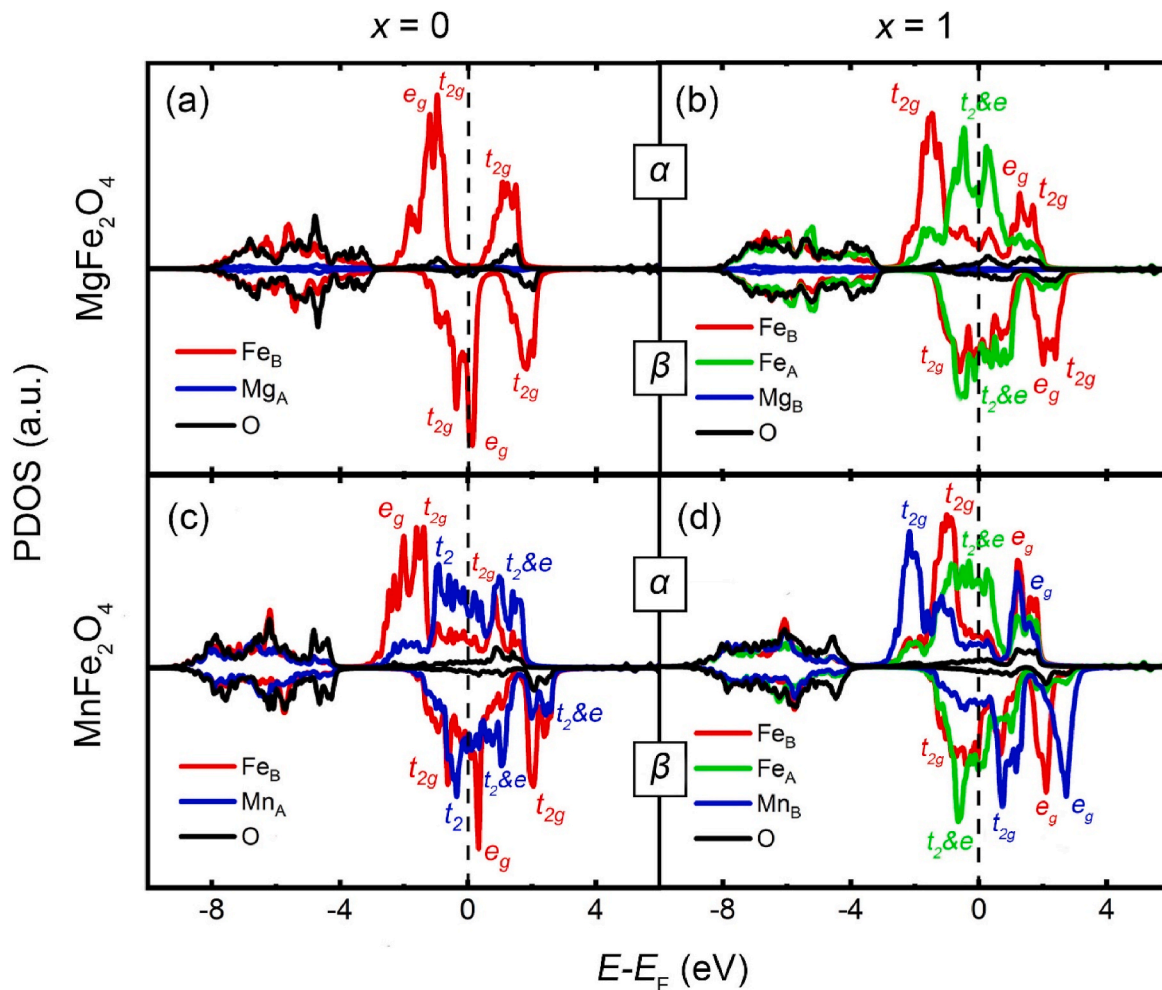


Fig. 5. PDOS per atom for MgFe_2O_4 and MnFe_2O_4 at inversion degrees 0 and 1.

predominantly below E_F , have lower energy than β channel states. For M in both ferrites, t_{2g} and e_g states at octahedral sites are more spread out in energy than t_2 and e states at tetrahedral sites.

Analysis of the PDOS in Fig. 3 shows the DOS near E_F is dominated by Fe states. There are also O electronic states near E_F , but their density is low. Therefore, the valence and conduction bands of these spinels are primarily composed of Fe 3d states. Our result is different from previous studies in which the valence and conduction bands of spinel ferrites were reported to be primarily of the O type [15,16]. Zn^{2+} and Cd^{2+} ions are very stable since their outer d orbitals are fully occupied. Therefore, their states are far below E_F , and have weak or no interaction with Fe 3d electrons.

Compared to the PDOS for M atoms in normal case, a clear rise in energy is found for PDOS of M atoms in the inverse case, *i.e.*, from -7.0 eV to -6.0 eV for ZnFe_2O_4 and from -9.0 eV to -8.0 eV for CdFe_2O_4 . Therefore, it is less likely for M atoms to occupy octahedral sites. Comparing the Fe PDOS in both cases, we can see that when Fe occupies tetrahedral sites, the overall energy in the inverse case is higher than that in the normal case, hence it is favorable for Fe to occupy the octahedral sites. From above analysis, we confirm that ZnFe_2O_4 and CdFe_2O_4 are normal spinels.

The PDOS for NiFe_2O_4 and CoFe_2O_4 at inversion degrees 0 and 1 is plotted in Fig. 4. In contrast to Fig. 3, in all scenarios, the electronic states near E_F have major contributions from both M and Fe. For O, almost all states lie far below E_F , and the O DOS near E_F is low, similar to that in Fig. 3. Therefore, the valence and conduction bands are not primarily of the O type.

In the $x = 0$ case, as shown in Fig. 4(a) and (c), the t_2 and e electronic states of M are very close in energy, and most states have energy $\leq E_F$. For Fe electronic states, there is a clear splitting between t_{2g} and e_g , with e_g states having lower energy. In CoFe_2O_4 , for Fe e_g states, α channel states contribute to the valence band, and β channel states pass through E_F . Fe t_{2g} states mainly contribute to the conduction band, with β channel t_{2g} states possessing higher energies. In NiFe_2O_4 , the Fe DOS in α channel has a similar distribution to that in β channels of CoFe_2O_4 , and *vice versa*.

The PDOS for $x = 1$ case is shown in Fig. 4(b) and (d). In contrast to the $x = 0$ case, M states now have evidently split t_{2g} and e_g states. t_{2g} states contribute to the valence band, and e_g states contribute to the conduction band, with an exception of β channel e_g states in NiFe_2O_4 , which are below E_F . For Fe_A states, t_2 and e states have almost the same distribution. However, the spin decomposed DOS of Fe_A is not symmetric: α channel states mainly contribute to the valence band, while β channel states largely contribute to the conduction band. Fe_B states are similar to those in the $x = 0$ case, but t_{2g} states have lower energies than e_g states. The overall energy of Fe states is lower than that of the $x = 0$ case, indicating that the system is more stable when Fe occupies A sites, hence further confirming NiFe_2O_4 and CoFe_2O_4 are inverse spinels.

Fig. 5 shows the PDOS of mixed spinel ferrites MgFe_2O_4 and MnFe_2O_4 . In MgFe_2O_4 , the Mg^{2+} ion does not have 3d electrons, demonstrating very scarce DOS. Most O states have energies far below E_F , and Fe states are predominant near E_F . In the normal case, the energy distribution of Fe e_g and t_{2g} states are complicated due to hybridization. α channel e_g states have lower energy than t_{2g} states, with formation of a gap between two t_{2g} bands, while β channel e_g states have energies

between two t_{2g} bands, passing through E_F . In the inverse case, for Fe_A , the t_2 and e states are close in energy and nearly symmetrical in α and β spin channels, with high density between -1.0 eV and $+1.0$ eV; for Fe_B , the e_g states sit between two t_{2g} bands, with α channel states forming a gap and β channel states passing through E_F .

For $MnFe_2O_4$, in the normal case, Fe states are similar to those of $MgFe_2O_4$. The t_2 and e states of Mn_A are closely distributed around E_F , with high densities from -2.0 eV to $+2.0$ eV. In the inverse case, Fe states are also analogous to that of $MgFe_2O_4$, except for e_g states of Fe_B , which have higher energy than t_{2g} bands and are no longer located between two t_{2g} bands. The Mn_B DOS shows clear splitting of t_{2g} and e_g states, which is also observed for M states in Figs. 3 and 4. Compared to $x = 0$, the β channel states have higher energy, and are mostly unoccupied (above E_F), while α channel states form a gap and are shifted to lower energies.

The electronic structure of mixed spinel $MgFe_2O_4$ would be a mixture of the normal and inverse cases. However, $MgFe_2O_4$ has an inversion degree $x \sim 0.9$ [34,35], and its PDOS would therefore exhibit more characteristics of the inverse type. For $MnFe_2O_4$, $x \sim 0.2$ [36,37], so its electronic states would be more of the normal type.

The PDOS calculations of these spinel ferrites contain a lot of information about their physical properties. For all investigated spinels, the DOS in the α and β channels is not symmetrical, giving rise to the ferrimagnetic property observed experimentally [40]. In addition, states passing through E_F contribute to conductivity of spinel ferrites [41,42]. In our DFT calculations, it is found that Fe and M atoms (except Mg) show clear splitting of t_{2g} and e_g states when occupying octahedral sites, while t_2 and e states are close when they occupy tetrahedral sites. Thus, the Jahn-Teller effect at octahedral sites is stronger than that at tetrahedral sites. In contrary to previous studies [15,16], the valence and conduction bands are not primarily of the O type, but are dominated by states of either Fe or both Fe and M. Careful examination of the PDOS for $ZnFe_2O_4$ and $CdFe_2O_4$ with a normal spinel structure shows that there is almost no overlap between M and Fe electronic states. The M states lie far below E_F , while Fe states are abundant near E_F . However, for inverse and mixed spinels, the M and Fe DOS have large overlaps, with both DOS lying near E_F . Therefore, the interaction between M and Fe states can serve as a criterion to predict the cation distribution of spinel ferrites. Weak or no interaction leads to a normal spinel structure, while strong interaction suggests the spinel has an inverse or mixed structure.

4. Conclusions

In this work, the thermodynamics and electronic structures of six spinel ferrites were examined to differentiate their spinel structures. The thermodynamic calculations were successful in predicting the spinel structure type of the investigated spinel ferrites, although there were discrepancies in the inversion degrees obtained from calculation and experiment for the mixed spinels. From the electronic structure analysis, it is found that when M and Fe atoms are at octahedral sites, the Jahn-Teller effect is stronger than that in tetrahedral sites. For all six spinel ferrites, the DOS near E_F has major contributions from either M and Fe or just Fe, while O DOS is low near E_F . Strong interaction between Fe and M DOS is a common characteristic for spinel ferrites with a mixed or inverse spinel structure, while weak or no interaction between these two suggests a normal spinel structure. Our results show that thermodynamic free energy of inversion combined with electronic structure calculations can provide strong guidance for determination of spinel structures for spinel ferrites.

Declaration of competing interest

The authors declare that they have no known competing financial interests or personal relationships that could have appeared to influence the work reported in this paper.

Acknowledgements

We would like to thank the financial support from the National Natural Science Foundation of China (Grant No.: 10974105), Shandong Province “Double-Hundred Talent Plan” Program (Grant No.: WST2018006), High-end foreign experts project of the Ministry of Science and Technology, China (Grant no.: G2022025015L, G2022025016L). Y. Q. Wang would also like to thank the financial support from the Taishan Scholar Program, and Qingdao International Center for Semiconductor Photoelectric Nanomaterials and Shandong Provincial University Key Laboratory of Optoelectrical Material Physics and Devices.

References

- [1] A. Soufi, H. Hajjaoui, R. Elmoubarki, M. Abdennouri, S. Qourzal, N. Barka, Spinel ferrites nanoparticles: synthesis methods and application in heterogeneous Fenton oxidation of organic pollutants - a review, *Appl. Surf. Sci. Adv.* 6 (2021), 100145.
- [2] E. Skliri, J. Miao, J. Xie, G. Liu, T. Salim, B. Liu, Q. Zhang, G.S. Armatas, Assembly and photochemical properties of mesoporous networks of spinel ferrite nanoparticles for environmental photocatalytic remediation, *Appl. Catal. B Environ.* 227 (2018) 330–339.
- [3] M. Li, Y. Xiong, X. Liu, X. Bo, Y. Zhang, C. Han, L. Guo, Facile synthesis of electrospun MFe_2O_4 ($M = Co, Ni, Cu, Mn$) spinel nanofibers with excellent electrocatalytic properties for oxygen evolution and hydrogen peroxide reduction, *Nanoscale* 7 (2015) 8920–8930.
- [4] V. Inglezakis, S. Pouloupoulos, Adsorption, Ion Exchange and Catalysis: Design of Operations and Environmental Applications, Elsevier, Amsterdam, 2006.
- [5] H. Qin, Y. He, P. Xu, D. Huang, Z. Wang, H. Wang, Z. Wang, Y. Zhao, Q. Tian, C. Wang, Spinel ferrites (MFe_2O_4): synthesis, improvement and catalytic application in environment and energy field, *Adv. Colloid Interface Sci.* 294 (2021), 102486.
- [6] P. Liu, H. He, G. Wei, X. Liang, F. Qi, F. Tan, W. Tan, J. Zhu, R. Zhu, Effect of Mn substitution on the promoted formaldehyde oxidation over spinel ferrite: catalyst characterization, performance and reaction mechanism, *Appl. Catal. B Environ.* 182 (2016) 476–484.
- [7] K.R. Sanchez-Lievanos, J.L. Stair, K.E. Knowles, Cation distribution in spinel ferrite nanocrystals: characterization, impact on their physical properties, and opportunities for synthetic control, *Inorg. Chem.* 60 (2021) 4291–4305.
- [8] L.I. Granone, A.C. Ulpe, L. Robben, S. Klimke, M. Jahns, F. Renz, T.M. Gering, T. Bredow, R. Dillert, D.W. Bahnemann, Effect of the degree of inversion on optical properties of spinel $ZnFe_2O_4$, *Phys. Chem. Chem. Phys.* 20 (2018), 28267.
- [9] P.I. Slick, E.P. Wohlfarth (Eds.), *Ferromagnetic Materials: A Handbook on the Properties of Magnetically Ordered Substances*, vol. 2, North-Holland, Amsterdam, 1980, pp. 189–242.
- [10] V.A.M. Brabers, K.H.J. Buschow (Eds.), *Handbook of Magnetic Materials*, vol. 8, Elsevier, Amsterdam, 1995, pp. 189–324.
- [11] J.K. Burdett, G.D. Price, S.L. Price, Role of the crystal-field theory in determining the structures of spinels, *J. Am. Chem. Soc.* 104 (1982) 92–95.
- [12] Y. Seminovski, P. Palacios, P. Wahnón, R. Grau-Crespo, Band gap control via tuning of inversion degree in $CdIn_2S_4$ spinel, *Appl. Phys. Lett.* 100 (2012), 102112.
- [13] A. Seko, F. Oba, I. Tanaka, Classification of spinel structures based on first-principles cluster expansion analysis, *Phys. Rev. B* 81 (2010), 054114.
- [14] D. Santos-Carballal, A. Roldan, R. Grau-Crespo, N.H. de Leeuw, First-principles study of the inversion thermodynamics and electronic structure of FeM_2X_4 (thio) spinels ($M = Cr, Mn, Co, Ni$; $X = O, S$), *Phys. Rev. B* 91 (2015), 195106.
- [15] J. Yao, X. Li, Y. Li, S. Le, Density functional theory investigations on the structure and electronic properties of normal spinel $ZnFe_2O_4$, *Integrated Ferroelectrics Int. J.* 145 (2013) 17–23.
- [16] Z. Szotek, W.M. Temmerman, D. Ködderitzsch, A. Svane, L. Petit, H. Winter, Electronic structures of normal and inverse spinel ferrites from first principles, *Phys. Rev. B* 74 (2006), 174431.
- [17] M.A. Rafiq, A. Javed, M.N. Rasul, M.A. Khan, A. Hussain, Understanding the structural, electronic, magnetic and optical properties of spinel MFe_2O_4 ($M = Mn, Co, Ni$) ferrites, *Ceram. Int.* 46 (2020) 4976–4983.
- [18] A. Azouaoui, M. El Haoua, S. Salmi, A. El Grini, N. Benzakour, A. Hourmatallah, K. Bouslykhane, Structural and magnetic properties of Cd-Co ferrites: density functional theory calculations and high-temperature series expansions, *J. Supercond. Nov. Magnetism* 33 (2020) 1831–1838.
- [19] D.J. Singh, R.C. Rai, J.L. Musfeldt, S. Auluck, N. Singh, P. Khalifah, S. McClure, D. G. Mandrus, Optical properties and electronic structure of spinel $ZnRh_2O_4$, *Chem. Mater.* 18 (2006) 2696–2700.
- [20] X. Shi, S.L. Bernasek, A. Selloni, Formation, electronic structure, and defects of Ni substituted spinel cobalt oxide: a DFT+U study, *J. Phys. Chem. C* 120 (2016) 14892–14898.
- [21] R.F.W. Bader, *Atoms in Molecules: A Quantum Theory*, Oxford University Press, Oxford, UK, 1990.
- [22] A. Navrotsky, O.J. Kleppa, The thermodynamics of cation distributions in simple spinels, *J. Inorg. Nucl. Chem.* 29 (1967) 2701–2714.
- [23] H. St, C. O'Neill, Temperature dependence of the cation distribution in zinc ferrite ($ZnFe_2O_4$) from powder XRD structural refinements, *Eur. J. Mineral* 4 (1992) 571–580.

- [24] S. Bid, S.K. Pradhan, Microstructure characterization and phase transformation kinetic study of mechano-synthesized non-stoichiometric CdFe_2O_4 by Rietveld's analysis, *Jpn. J. Appl. Phys.* 43 (2004) 5455–5464.
- [25] S. Ayyappan, J. Philip, B. Raj, A facile method to control the size and magnetic properties of CoFe_2O_4 nanoparticles, *Mater. Chem. Phys.* 115 (2009) 712–717.
- [26] S. Bid, P. Sahu, S.K. Pradhan, Microstructure characterization of mechano-synthesized nanocrystalline NiFe_2O_4 by Rietveld's analysis, *Physica E* 39 (2007) 175–184.
- [27] K.A. Shaw, E. Lochner, D.M. Lind, J.F. Anderson, M. Kuhn, U. Diebold, Magnesium outdiffusion through magnetite films grown on magnesium oxide (001), *J. Appl. Phys.* 81 (1997) 5176.
- [28] S.R. Patade, D.D. Andhare, S.B. Somvanshi, S.A. Jadhav, M.V. Khedkar, K. M. Jadhav, Self-heating evaluation of superparamagnetic MnFe_2O_4 nanoparticles for magnetic fluid hyperthermia application towards cancer treatment, *Ceram. Int.* 46 (2020) 25576–25583.
- [29] J. Zhou, J. Ma, C. Sun, L. Xie, Z. Zhao, H. Tian, Low-temperature synthesis of NiFe_2O_4 by a hydrothermal method, *J. Am. Ceram. Soc.* 88 (2005) 3535–3537.
- [30] M. Srivastava, A.K. Ojha, S. Chaubey, A. Materny, Synthesis and optical characterization of nanocrystalline NiFe_2O_4 structures, *J. Alloys Compd.* 481 (2009) 515–519.
- [31] J.L.M. de Vidales, A. López-Delgado, E. Vila, F.A. Lopez, The effect of the starting solution on the physico-chemical properties of zinc ferrite synthesized at low temperature, *J. Alloys Compd.* 287 (1999) 276–283.
- [32] V. Vasanthi, A. Shanmugavani, C. Sanjeeviraja, R. Kalai Selvan, Microwave assisted combustion synthesis of CdFe_2O_4 : magnetic and electrical properties, *J. Magn. Mater.* 324 (2012) 2100–2107.
- [33] N. Ballarini, F. Cavani, S. Passeri, L. Pesaresi, A.F. Lee, K. Wilson, Phenol methylation over nanoparticulate CoFe_2O_4 inverse spinel catalysts: the effect of morphology on catalytic performance, *Appl. Catal. Gen.* 366 (2009) 184–192.
- [34] H. St, C. O'Neill, H. Annersten, D. Virgo, The temperature dependence of the cation distribution in magnesioferrite (MgFe_2O_4) from powder XRD structural refinements and Mössbauer spectroscopy, *Am. Mineral.* 77 (1992) 725–740.
- [35] J.P. Singh, S.O. Won, W.C. Lim, I.J. Lee, K.H. Chae, Electronic structure studies of chemically synthesized MgFe_2O_4 nanoparticles, *J. Mol. Struct.* 1108 (2016) 444–450.
- [36] A. Doaga, A.M. Cojocariu, W. Amin, F. Heib, P. Bender, R. Hempelmann, O. F. Caltun, Synthesis and characterizations of manganese ferrites for hyperthermia applications, *Mater. Chem. Phys.* 143 (2013) 305–310.
- [37] K. Vamvakidis, M. Katsikini, D. Sakellari, E.C. Paloura, O. Kalogiroub, C. Dendrinou-Samara, Reducing the inversion degree of MnFe_2O_4 nanoparticles through synthesis to enhance magnetization: evaluation of their ^1H NMR relaxation and heating efficiency, *Dalton Trans.* 43 (2014) 12754–12765.
- [38] I.H. Jung, S.A. Decterov, A.D. Pelton, Critical thermodynamic evaluation and optimization of the Fe-Mg-O system, *J. Phys. Chem. Solid.* 65 (2004) 1683–1695.
- [39] I.H. Jung, S.A. Decterov, A.D. Pelton, H.M. Kim, Y.B. Kang, Thermodynamic evaluation and modeling of the Fe-Co-O system, *Acta Mater.* 52 (2004) 507–519.
- [40] F.G. da Silva, J. Depeyrot, A.F.C. Campos, R. Aquino, D. Fiorani, D. Peddis, Structural and magnetic properties of spinel ferrite nanoparticles, *J. Nanosci. Nanotechnol.* 19 (2019) 4888–4902.
- [41] A.S. Fawzi, A.D. Sheikh, V.L. Mathe, Structural, dielectric properties and AC conductivity of $\text{Ni}_{(1-x)}\text{Zn}_x\text{Fe}_2\text{O}_4$ spinel ferrites, *J. Alloys Compd.* 502 (2010) 231–237.
- [42] R. Qindeel, N.H. Alonizan, Structural, dielectric and magnetic properties of cobalt based spinel ferrites, *Curr. Appl. Phys.* 18 (2018) 519–525.